



Fabrication of W-4.9Ni-2.1Fe /Y₂O₃ composites by powder metallurgy route: effect of Ca impurity on microstructure and mechanical properties

Narjes Saadatmandfard¹, Gholam Hussain Borhani^{1*}, Seyed Akbar Miresmaeili Hafdani¹, Seyed Masoud Barekat²

¹Department of Materials Engineering, Malek-Ashtar University of Technology, Isfahan, Iran

²Department of Materials Engineering, Malek-Ashtar University of Technology, Tehran, Iran

Received: 2022-02-19; Revised February: 2022-09-09; Accepted for publication: 2022-11-23

* Corresponding author: Gholam Hussain Borhani (Borhani_g@yahoo.co.uk)

© Published by Shahid Chamran University of Ahvaz.

Abstract

In this article an attempt is made to prepare W-4.9Ni-2.1Fe alloy and W-4.9Ni-2.1Fe/Y₂O₃ composite by powder metallurgy route. A detailed experimental study was performed to characterize the influence of ceramic particles Y₂O₃ and Ca impurities on microstructure and mechanical properties. The raw powder materials were mixed and then mechanically milled for 3h in Ar atmosphere. Y₂O₃ powder was added to milled powders in the last 30 min of milling. The milled powders were cold compacted at 300 MPa in cylindrical form and then subjected to liquid phase sintering at 1470 °C in dried Hydrogen atmosphere. The sintered samples were characterized for microstructure studies (SEM equipped with EDS), physical properties (Density and Young's modulus) and mechanical properties (Rockwell hardness and Compressive strength). All sintered samples exhibited sintered density in the range of 15.4 to

16 g/cm³ (94 to 99 % relative density). Y₂O₃ and Ca impurities had a controlled role on W grain size growth. The compressive strength of composite samples increased up to 800MPa for W-4.9Ni-2.1Fe-1 Y₂O₃. Uniform distribution of W spheroids in Ni-Fe matrix was observed in sintered samples. The mean grain size of sintered samples varied in the range of 12 to 30 μm.

Keywords: Powder metallurgy, W-Ni-Fe alloy, Y₂O₃, Ca impurity, Microstructure, Mechanical properties.

1. Introduction

Tungsten heavy alloys (WHAs) have W particles distributed in the ductile binder such as transition metals including: Fe, Ni, Co, Cu, etc. WHAs with up to 90 wt. % W have unique properties such as high density (17-18.25 g/cm³), high strength (ultimate strength up to 1000 MPa) and reasonable elongation (20-30%) [1], [2]. In WHAs, the γ phase has the lowest melting point and the best Ni to Fe ratio of 7:3 [3]. WHA is usually produced through liquid phase sintering and, is known for its coarse grains and non-uniform structure. Several methods can be applied to modify tungsten powder for limiting the grain growth of tungsten during sintering. These methods include mixing of tungsten powder with molybdenum, rhenium and tantalum elements or addition of ceramic particles [3], [4]. The CaWO₄ is introduced as unwanted impurity in W powder, but it is reported that some unreduced CaWO₄ particles (about of 2.2 wt. %) restrain the grain growth and mass transport in the liquid phase sintering processing [5]. Addition of nonmetallic inclusions (oxides & carbides) to tungsten alloys in the range of 0.1 to 0.4 wt. % was reported to control the grain growth [6], [7]. The presence of ceramic particles (due to very high melting point) in W-W grain boundaries impede the Tungsten grain growth, followed by increase in tensile strength and fracture toughness [8], [9]. It has been observed that with the addition of ceramic particles the strength of W-Ni-Fe-Y₂O₃ composites is first reduced and then increased [8]. In 2015, an increase in the Young's modulus was reported with the addition of 1 to 2 wt. % of Y₂O₃ [10]. The effect of adding TiC particles to tungsten heavy alloys was investigated [11]. The results showed that the addition of TiC can affect the mechanical properties of WHAs by placing them between W-W boundaries and preventing grain growth. A. Pathak et al. [12] investigated the effect of adding TiC to Tungsten. Addition of 5 wt. % TiC resulted in better microstructural refinement. Agglomeration of TiC particles between W grains causes finer grains and consequently increases the strength and fracture toughness. In the present study, an attempt was made to investigate the role of ceramic

particles in the presence of minor Ca impurities on microstructures, physical and mechanical properties of W-Ni-Fe/ Y_2O_3 composites.

2. Materials and Methods

Elemental powders of conventional tungsten (average particle size: 3 μm , and purity: +99.5%), nickel (average particle size: 22 μm , and purity: +99.95%), iron (average particle size: 24 μm and purity: +99.9%), Y_2O_3 (average particle size: 33 nm and purity: 99.99%) were used as starting materials. **Fig. 1** shows the secondary electron (SE) micrographs of the elemental powders. The composition of W, Ni and Fe elemental powders were evaluated by ICP method as reported in **Table 1**.

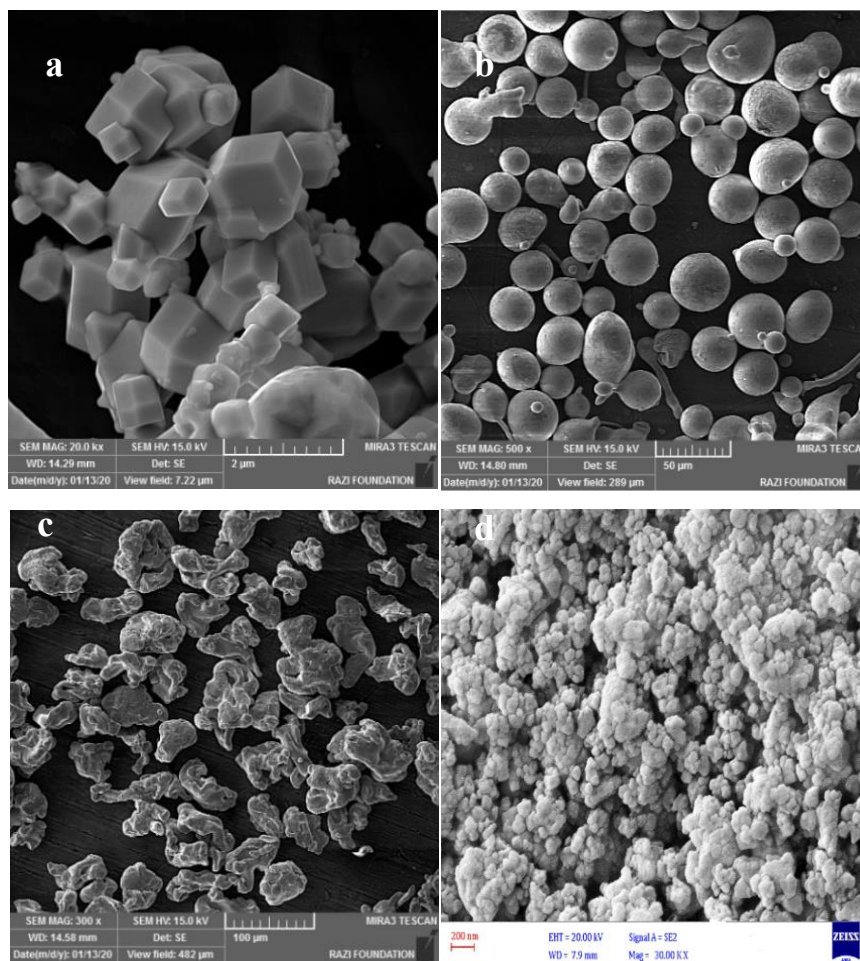


Fig. 1: Morphology of a) W, b) Ni, c) Fe, d) Y_2O_3 powders

Table 1: Chemical composition of W, Ni and Fe elemental powders

Elements/ powder	Fe	Ni	W	Pb	Mg	Co	Na	Ca
W	213 ppm	-	Bal.	95 ppm	141 ppm	377 ppm	378 ppm	0.2%
Ni	31.3 ppm	Bal.	-	-	171 ppm	0.154 ppm	-	182 ppm
Fe	Bal.	179 ppm	-	-	83 ppm	35 ppm	407 ppm	196 ppm

Powder mixture with chemical composition of 93W-4.9Ni-2.1Fe (wt. %) was blended for 1h and then mechanically milled with rotational speed of 300 rpm and ball to powder weight ratio of 10:1 for 3h; 1 wt. % of Y₂O₃ powder was added to the milled powder and the milling continued for another 30 min. Milled powders were compacted through uniaxial hydraulic press up to 300 MPa in order to obtain cylindrical compact of 15 mm diameter and 20 mm height, cylindrical height of 15 mm diameter and 20 mm height. These compacts (composite and alloy) were consolidated in a tube furnace at 1470 °C for 30 min in a dry hydrogen atmosphere at a flow rate of 1.44 L/min. Density of the sintered samples was measured through Archimedes' water displacement method. Hardness of all samples was evaluated through Rockwell hardness technique. The compressive strength and Young's modulus of sintered samples were evaluated by mechanical tensile testing machine (SANTAM) and ultrasonic elastic modulus tester, respectively. In order to obtain fracture surfaces, a setup was designed to pull the sample in different uniaxial directions, tilt the sample reached fracture mode. SEM of specimens was performed to investigate average grain size (Martin diameter) and fractography of WHAs samples. The Young's modulus was determined using the Eq. 1:

$$E = \rho V^2 \quad \text{Eq. 1}$$

Where, E is the Young's modulus, V is the sound speed in material and ρ is the sample density.

3. Results and Discussion

a) Microstructure characterization

Fig. 2 shows the secondary electron (SE) micrographs and EDS analysis of mixed elemental powders of tungsten, nickel and iron. According to EDS results, not only were all the mixed elemental powders recognized but some minor calcium peaks were also identified. The microstructural representation of sintered samples is illustrated in **Fig. 3**. The results showed that the molten gamma phase has formed and flowed around the tungsten grains. Average grain

size of W-4.9Ni-2.1Fe and W-4.9Ni-2.1Fe-1Y₂O₃ were calculated as 30 μ m and 12 μ m, respectively.

The W-4.9Ni-2.1Fe composition was sintered at 1480 °C for 1.5 h in hydrogen atmosphere. The alloys microstructure investigated by Pathak et al. showed the average grain size increased to 46 μ m after sintering at 1480 °C [13]. This indicates that the grain size of the present experiment sintered at 1470 °C has decreased by 36%. Yet, the presence of Y₂O₃ has decreased the grain size by further 60% (**Fig. 3-b**). The presence of Y₂O₃ controlled the grain size during sintering and decreased the grain size. **Table 2** presents a comparison of grain size in present study with those of previous studies.

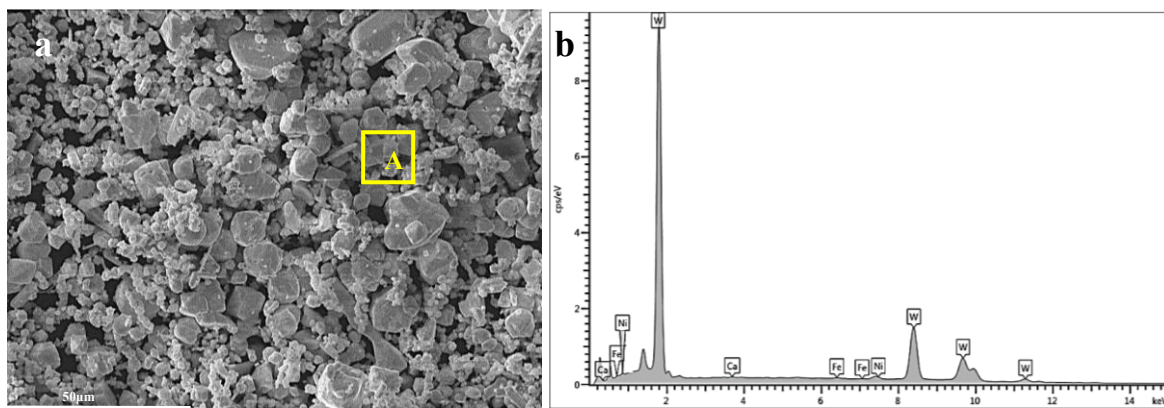


Fig. 2: Mixed powder: a) morphology, and b) EDS analysis

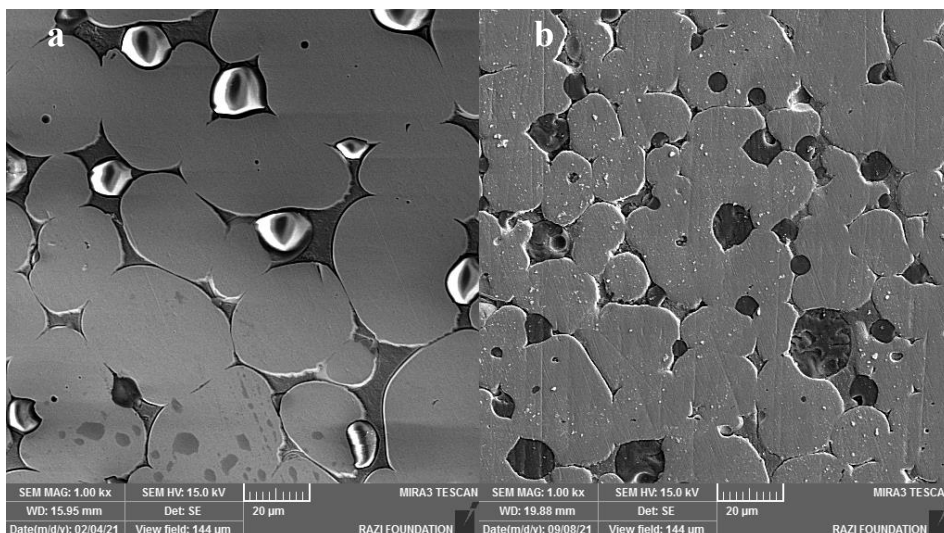
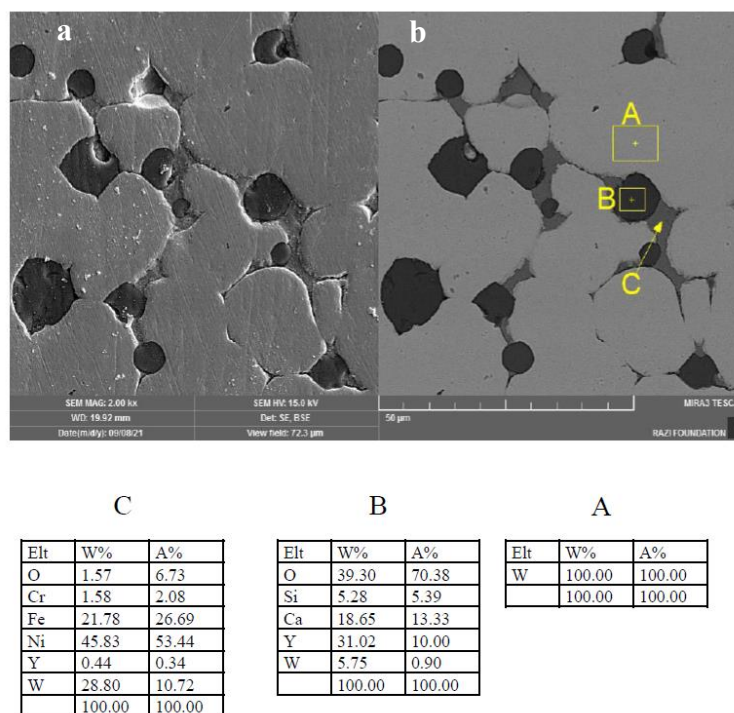


Fig. 3: SEM of a) W-4.9Ni-2.1Fe alloys, b) W-4.9Ni-2.1Fe-1Y₂O₃ specimens

Table 2: Grain size in present study and previous study

Composition	Sintering condition	Grain size (μm)	Ref.
93W-4.9Ni-2.1Fe	1480°C- 1.5h -H ₂	46	[13]
93W-5.6Ni-1.4Fe	1485°C-1h-H ₂	40	[14]
93W-4.9Ni-2.1Fe	1470°C-1 h-H ₂	30	Present study

There are some silver-colored particles (**Fig. 3-a**) which were not observed in the mixture of raw powders. This finding was consistent with Erol's research [15] indicating that these particles form a compound with Si. **Fig. 4** shows the W-4.9Ni-2.1Fe-1Y₂O₃ microstructure with EDS results. It shows the uniform distribution of agglomerated Y₂O₃ (B) and γ liquid phase (C). Some other impurities with dark gray color are also visible (B), which are mixed with Y₂O₃ particles. The EDS results indicate the presence of Si and Ca compounds within the specimen. Ca compounds are usually present in commercial tungsten powder, this is because of incomplete washing of tungstic acid during tungsten reduction. Si and Cr might have entered the matrix during MA process. The presence of Cr₂O₃ is the result of balls and stainless steel container wearing during mechanical milling [16]. These impurities appear to have some effects on preventing the grain growth (**Table 2**). Although the presence of impurities can have a negative effect on the properties of the sample, it can be effective in reducing grain growth.

**Fig. 4:** SEM image of a) SE, b) BSE and EDS analysis of W-4.9Ni-2.1Fe-1Y₂O₃

The presence of Y_2O_3 has not only decreased the grain growth, but it has also modified the properties of W-4.9Ni-2.1Fe-1 Y_2O_3 composites.

b) Physical and mechanical properties

Results of density, grain size, physical and mechanical properties of sintered specimens are reported in **Tables 3** and **Table 4**.

Table 3: The density measurements of sintered samples

Density	W-4.9Ni-2.1Fe	W-4.9Ni-2.1Fe/1 Y_2O_3
Theoretical (g/cm^3)	16.47	16.14
Apparent (g/cm^3)	8.98	10.93
Sintered (g/cm^3)	15.49	16
Relative %	94 %	99.1 %

Table 4: The average grain size and mechanical properties of sintered samples

Composition	Compressive strength (MPa)	H (HRC)	Grain size (μm)	V (m/s)	E (GPa)
W-4.9Ni-2.1Fe	780	24 \pm 2	30	4585	368
W-4.9Ni-2.1Fe-1 Y_2O_3	850	27 \pm 1	12	4950	418

It has been observed that the density of W-4.9Ni-2.1Fe/1 Y_2O_3 composite has improved compared to W-4.9Ni-2.1Fe alloy. This could be due to the mixture of nano-sized Y_2O_3 particles within the tungsten powders, which has filled the cavities and increased the density [8]. Owing to the use of Y_2O_3 particles (with the density of $5.01 g/cm^3$) and the presence of Ca compound, the theoretical density has decreased compared to the W-4.9Ni-2.1Fe composition. The relative density reported in Table 2 has been calculated with existing impurities included in the mixture. In fact, the impurity in the microstructure is identified as calcium tungstate ($CaWO_4$) with density of $6.12 g/cm^3$. The value of theoretical density is calculated $16.47 g/cm^3$. With the addition of Y_2O_3 the theoretical density is decreased to $16.14 g/cm^3$. The hardness of samples matched well with previous researches [13], [17]. Due to the optimization of the amount of Y_2O_3 particles, adding 1 wt. % of Y_2O_3 does not have a significant effect on the hardness. The hardness of pure tungsten is reported between 30 and 58 HRC [16]. The decrease in hardness of W-4.9Ni-2.1Fe alloys is due to the flow of the optimum gamma phase between the tungsten grains, which has led to an increase in the toughness [18]. It is reported that the

decrease in hardness can also be due to the presence of Ca impurity[15]. The compressive strength of W-4.9Ni-2.1Fe and W-4.9Ni-2.1Fe-1Y₂O₃ samples was calculated as 780 and 850 MPa, respectively. The increase in compressive strength of the samples can be due to two reasons: (1) Y₂O₃ particles located at W grain boundaries and (2) the presence of impurities of Ca particles, preventing the grain growth. These phenomena are also observed and reported by other researchers [5], [19]. Based on the present research it can be pointed out that using commercial powders along with some nanometer-sized ceramics can lead to the production of samples with optimal mechanical properties. This finding makes the production of these samples economically viable and responsive to industrial applications in terms of physical and mechanical properties. The SEM fractography of W-4.9Ni-2.1Fe alloys and W-4.9Ni-2.1Fe-1Y₂O₃ composite are shown in **Fig. 5**. The presence of Y₂O₃ had no significant effect on the fractography observations. There are several visible intergranular fractures in both cases that are shown with arrows. These fractures are a sign of ductile fracture, along with intergranular fracture. In general, it can be concluded that the presence of impurities and Y₂O₃ particles has created a mixed mode fracture surface, which is a combination of ductile and brittle fracture mechanisms.

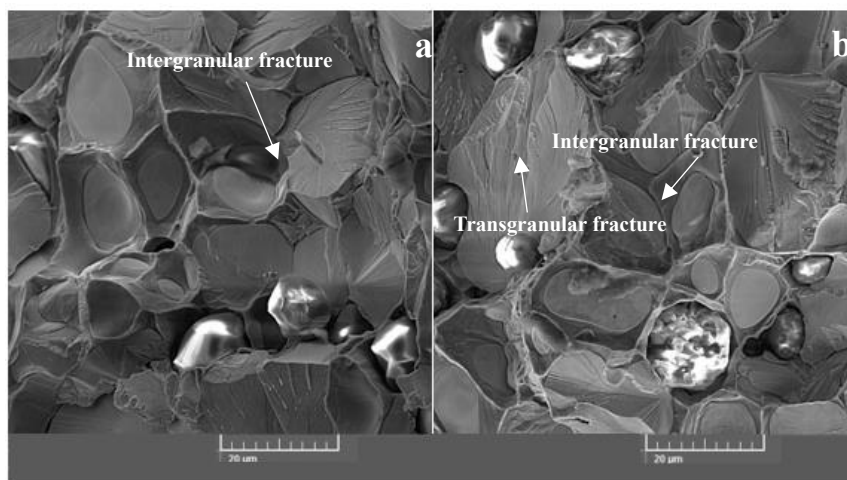


Fig. 5: Fractography of a) W-4.9Ni-2.1Fe alloys, b) W-4.9Ni-2.1Fe-1Y₂O₃ specimens

The presence of Y₂O₃ has modified the mechanical properties of W-4.9Ni-2.1Fe-1Y₂O₃ composite. The Young's modulus of the W-4.9Ni-2.1Fe-1Y₂O₃ composites has increased by 12% compared to W-4.9Ni-2.1Fe alloys (418 GPa). The value of the Young's modulus is in accordance with the results reported for different tungsten heavy alloy-based composites[12], [20], [21]. The Young's modulus of pure tungsten is approximately 390 to 410 GPa [15]. The application of different processes for tungsten alloys fabrication such as addition of ceramic

particles, milling, etc. has increased the Young's modulus [22]. This is the result of grain size reduction and microstructure modification.

4. Conclusions

In this article an attempt is made to prepare W-4.9Ni-2.1Fe alloy and W-4.9Ni-2.1Fe/Y₂O₃ composite by powder metallurgy route. Effect of Y₂O₃ ceramic particles and Ca impurities on microstructure and mechanical properties was investigated. Results showed addition of Y₂O₃ can improve the microstructure and mechanical properties of commercial tungsten heavy alloys. The Y₂O₃ particles were located between the tungsten grains and reduced the grain average size by 60%. Lastly, the values of strength and hardness have also improved. The addition of 1 wt. % Y₂O₃ increased the Young's modulus by about 12% (as compared to the sintered sample without ceramic particles). Calcium compounds and other impurities acted as minor inhibitor to control the grain size.

References

- [1] N. Senthilnathan, A. Raja Annamalai, and G. Venkatachalam, "Sintering of Tungsten and Tungsten Heavy Alloys of W–Ni–Fe and W–Ni–Cu: A Review," *Trans. Indian Inst. Met.*, vol. 70, no. 5, pp. 1161–1176, Jul. 2017, doi: 10.1007/s12666-016-0936-2.
- [2] Y. Wu, R. M. German, B. Marx, P. Suri, and R. Bollina, "Comparison of densification and distortion behaviors of W-Ni-Cu and W-Ni-Fe heavy alloys in liquid-phase sintering," *J. Mater. Sci.*, vol. 38, no. 10, pp. 2271–2281, 2003, doi: 10.1023/A:1023725508608.
- [3] M. Debata, T. S. Acharya, P. Sengupta, P. P. Acharya, S. Bajpai, and K. Jayasankar, "Effect of high energy ball milling on structure and properties of 95W-3.5Ni-1.5Fe heavy alloys," *Int. J. Refract. Met. Hard Mater.*, vol. 69, pp. 170–179, Dec. 2017, doi: 10.1016/j.ijrmhm.2017.08.007.
- [4] V. N. Chuvil'deev *et al.*, "Impact of mechanical activation on sintering kinetics and mechanical properties of ultrafine-grained 95W-Ni-Fe tungsten heavy alloys," *J. Alloys Compd.*, vol. 773, pp. 666–688, Jan. 2019, doi: 10.1016/j.jallcom.2018.09.176.
- [5] M. Erol, M. Erdoğan, and İ. Karakaya, "Effects of fabrication method on initial powder characteristics and liquid phase sintering behaviour of tungsten," *Int. J. Refract. Met. Hard Mater.*, vol. 77, pp. 82–89, Dec. 2018, doi: 10.1016/j.ijrmhm.2018.07.012.

- [6] R. V. Minakova, L. G. Bazhenova, P. A. Verkhovodov, O. P. Kolchin, L. P. Nedelyaeva, and A. V. Tolstunov, "Effect of impurity element substitution on the failure behavior of a W-Ni-Fe alloy," *Sov. Powder Metall. Met. Ceram.*, vol. 22, no. 11, pp. 932–937, Nov. 1983, doi: 10.1007/BF00805553.
- [7] J. Zou *et al.*, "Effect of HfC addition on the microstructure and properties of W–4.9Ni–2.1Fe heavy alloys," *J. Alloys Compd.*, vol. 872, p. 159683, Aug. 2021, doi: 10.1016/j.jallcom.2021.159683.
- [8] H. J. Ryu and S. H. Hong, "Fabrication and properties of mechanically alloyed oxide-dispersed tungsten heavy alloys," *Mater. Sci. Eng. A*, vol. 363, no. 1–2, pp. 179–184, Dec. 2003, doi: 10.1016/S0921-5093(03)00641-5.
- [9] N. K. Çalışkan, N. Durlu, and Ş. Bor, "Swaging of liquid phase sintered 90W–7Ni–3Fe tungsten heavy alloy," *Int. J. Refract. Met. Hard Mater.*, vol. 36, pp. 260–264, Jan. 2013, doi: 10.1016/j.ijrmhm.2012.10.001.
- [10] Z. Jiao, R. Kang, Z. Dong, and J. Guo, "Microstructure characterization of W-Ni-Fe heavy alloys with optimized metallographic preparation method," *Int. J. Refract. Met. Hard Mater.*, vol. 80, pp. 114–122, Apr. 2019, doi: 10.1016/j.ijrmhm.2019.01.011.
- [11] "Preparation and characterization of nano-sized TiC powder by sol gel processing TT - بررسی عوامل موثر بر سنتز کاربید تیتانیوم نانوساختار به روش سل ژل," *iut-jame*, vol. 32, no. 2, pp. 13–24, 2013. [Online]. Available: <http://jame.iut.ac.ir/article-1-556-en.html>
- [12] E. Tejado, A. Martin, and J. Y. Pastor, "Effect of Ti and TiC alloyants on the mechanical properties of W-based armour materials," *J. Nucl. Mater.*, vol. 514, pp. 238–246, Feb. 2019, doi: 10.1016/j.jnucmat.2018.12.001.
- [13] A. Pathak, A. Panchal, T. K. Nandy, and A. K. Singh, "Ternary W-Ni-Fe tungsten heavy alloys: A first principles and experimental investigations," *Int. J. Refract. Met. Hard Mater.*, vol. 75, pp. 43–49, Sep. 2018, doi: 10.1016/j.ijrmhm.2018.03.011.
- [14] H. J. Ryu, S. H. Hong, and W. H. Baek, "Microstructure and mechanical properties of mechanically alloyed and solid-state sintered tungsten heavy alloys," *Mater. Sci. Eng. A*, vol. 291, no. 1–2, pp. 91–96, Oct. 2000, doi: 10.1016/S0921-5093(00)00968-0.
- [15] M. A. M. Erol, "Liquid phase sintering characteristics of tungsten powder obtained by electrochemical reduction techniques," *Ankara Yildirim Beyazit Univ.*, 2017.

- [16] Y. Han, J. Fan, T. Liu, H. Cheng, and J. Tian, “The effect of trace nickel additive and ball milling treatment on the near-full densification behavior of ultrafine tungsten powder,” *Int. J. Refract. Met. Hard Mater.*, vol. 34, pp. 18–26, Sep. 2012, doi: 10.1016/j.ijrmhm.2012.02.014.
- [17] X. Gong, J. L. Fan, F. Ding, M. Song, and B. Y. Huang, “Effect of tungsten content on microstructure and quasi-static tensile fracture characteristics of rapidly hot-extruded W–Ni–Fe alloys,” *Int. J. Refract. Met. Hard Mater.*, vol. 30, no. 1, pp. 71–77, Jan. 2012, doi: 10.1016/j.ijrmhm.2011.06.014.
- [18] R. Osama, W. Elthalabawy, G. Abdo, and M. Sallam, “Effect of Limited Additions of Y₂O₃, ZrO₂ and Al₂O₃ on the Mechanical and Microstructure Characteristics of Tungsten Heavy Alloys,” *Int. Conf. Aerosp. Sci. Aviat. Technol.*, vol. 15, no. AEROSPACE SCIENCES, pp. 1–14, May 2013, doi: 10.21608/asat.2013.22109.
- [19] V. R. Talekar, A. Patra, S. K. Sahoo, S. K. Karak, and B. Mishra, “Fabrication and characterization of nano-Y₂O₃, Al₂O₃, La₂O₃ dispersed mechanically alloyed and liquid phase sintered W Ni for structural application,” *Int. J. Refract. Met. Hard Mater.*, vol. 82, pp. 183–198, Aug. 2019, doi: 10.1016/j.ijrmhm.2019.03.027.
- [20] K. Hu, X. Li, X. Ai, S. Qu, and Y. Li, “Fabrication, characterization, and mechanical properties of 93W–4.9Ni–2.1Fe/95W–2.8Ni–1.2Fe–1Al₂O₃ heavy alloy composites,” *Mater. Sci. Eng. A*, vol. 636, pp. 452–458, Jun. 2015, doi: 10.1016/j.msea.2015.04.026.
- [21] W. R. Lu, C. Y. Gao, and Y. L. Ke, “Constitutive modeling of two-phase metallic composites with application to tungsten-based composite 93W–4.9Ni–2.1Fe,” *Mater. Sci. Eng. A*, vol. 592, pp. 136–142, Jan. 2014, doi: 10.1016/j.msea.2013.11.007.
- [22] Y. Chen, Y. C. Wu, F. W. Yu, and J. L. Chen, “Microstructure and mechanical properties of tungsten composites co-strengthened by dispersed TiC and La₂O₃ particles,” *Int. J. Refract. Met. Hard Mater.*, vol. 26, no. 6, pp. 525–529, Nov. 2008, doi: 10.1016/j.ijrmhm.2007.12.004.